electronics

MDPI

Article

Generalized Filter Bank Orthogonal Frequency Division Multiplexing Systems for 6G

Yu Xin [1,2], Tong Bao [1,2], Jian Hua [1,2] and Hongming Zhang [3,*]

[1] State Key Laboratory of Mobile Network and Mobile Multimedia Technology, Shenzhen 518055, China; xin.yu@zte.com.cn (Y.X.); bao.tong@zte.com.cn (T.B.); hua.jian2@zte.com.cn (J.H.)
[2] ZTE Corporation, Shenzhen 518057, China
[3] School of Information and Communication Engineering, Beijing University of Posts and Telecommunications, Beijing 100876, China
* Correspondence: zhanghm@bupt.edu.cn

Abstract: In this study, generalized filter bank orthogonal frequency division multiplexing (GFB-OFDM) is proposed for 6G. In order to meet the different requirements of various scenarios in 6G, a unified structure of GFB-OFDM is designed by adopting the flexible capabilities of suitable transmission modules. In the proposed GFB-OFDM system, the coexistence of different numerologies in different sub-bands and/or the coexistence of single-carrier and multi-carrier waveforms are achieved for adjusting different scenarios in 6G. Finally, simulation results are provided to validate the BER performance of GFB-OFDM, showing that it is capable of achieving a comparable BER performance and much more flexible transmissions compared with the classic OFDM systems.

Keywords: 6G; waveform design; OFDM; FB-OFDM

Citation: Xin, Y.; Bao, T.; Hua, J.; Zhang, H. Generalized Filter Bank Orthogonal Frequency Division Multiplexing Systems for 6G. *Electronics* **2024**, *13*, 3006. https://doi.org/10.3390/electronics13153006

Academic Editor: Adão Silva

Received: 29 April 2024
Revised: 19 June 2024
Accepted: 21 June 2024
Published: 30 July 2024

1. Introduction

In the future, more and more complex application scenarios will emerge in sixth-generation (6G) cellular networks than 5G, and the requirements for different application scenarios will also vary by different performance indicators. For some special application scenarios, it is necessary to design new techniques for the air interface, especially the underlying waveform to ensure good performance, such as spectral and energy efficiency, bit error rate, and so on. In the future, there will also be the coexistence of multiple scenarios and rapid switching among different application scenarios in 6G, such as the integration of space–ground-based networks, the integration of industrial control applications, and the rapid switching between high-speed and low-speed mobile communications. However, a single-waveform solution can hardly meet the requirements of various 6G application scenarios [1,2].

Orthogonal frequency division multiplexing (OFDM) and DFT spread OFDM (DFT-s-OFDM) are supported in state-of-the-art wireless communication standards, such as 3GPP LTE and 5G NR standards families. OFDM is widely accepted due to its advantages of robustness against multi-path fading channels and relatively low complexity in both transmitters and receivers. However, OFDM suffers from poor spectral efficiency, which is partly caused by the high out-of-band emission (OOBE) from the side lobes. In addition, a high peak-to-average power ratio (PAPR) is another drawback for OFDM, so DFT-s-OFDM is used in the uplink to meet the requirements of high energy efficiency. It can be readily shown that a single-waveform scheme cannot easily meet the requirements of different scenarios in 5G, not to mention 6G. In this case, in order to effectively ensure performance in different scenarios, it is necessary to propose a new waveform that can meet the requirements of different scenarios with low complexity. A feasible solution in 5G is to support a set of numerologies; meanwhile, different waveform structures with flexible parameter configuration capabilities should also be supported to meet the

requirements of different scenarios, so as to realize the goal of supporting multiple scenarios and switching flexibly among different scenarios [3]. In this way, for each 5G deployment option, a given OFDM numerology, e.g., a set of the pre-defined subcarrier spacing, the predefined scaling factor, and the pre-defined cyclic-prefix duration, is used for generating the OFDM waveforms.

In order to solve the problems mentioned above, research has been conducted. In [4], different numerology sets are configured with OFDM, where the out-of-band radiation under configurations of different subcarrier spacing is observed, showing severe inter-subcarrier interference (ICI), which is difficult to effectively eliminate. Furthermore, when the length of the filter is fixed, larger subcarrier spacing leads to a slower speed of attenuation in the side lobes, which causes higher out-of-band radiation. In this case, if OFDM waveforms with different subcarrier configurations are sequentially set in the frequency band, ICI between the subcarriers with different spacing settings will be the main obstacle to demodulation in the receiver. This type of interference is also called inter-numerology interference (INI). The authors of [4] proposed a solution for INI by using frequency domain protection intervals, where zero bit streams are used. Similarly, the authors of [5] pointed out that the OFDM waveform should use as large a subcarrier spacing (SCS) as possible when selecting different numerology sets (mainly for subcarrier spacing) configurations, while taking into account the impact of Doppler frequency offset and phase noise. The time-domain windowing is proposed in [5] to deal with this kind of INI, with the goal of constraining out-of-band radiation and reducing the signal-to-interference ratio (SIR) in the continuous subcarriers of the target frequency band. This method of adding window function constraints to the continuous symbol edges formed by different SCS configurations essentially constitutes a windowed OFDM (W-OFDM) scheme. In addition, the authors of [6] explicitly addressed the INI problem when W-OFDM waveforms were loaded with different parameter sets and proposed a method of dividing sub-bands and performing sub-band filtering to achieve the purpose of interference cancellation. This scheme divides the available frequency bands into several sub-bands, with different SCS and cyclic prefix (CP) lengths configured between adjacent sub-bands. However, dividing different SCS into different frequency domain sub-bands can result in an inconsistent frame structure due to differences in the time-domain symbol lengths.

Another type of solution to achieve the requirements of 6G different scenarios is to apply multiple waveforms to configure different numerology sets, and this type of multi-waveform coexistence design is also known as green coexistence. In [7], a green coexistence design of CP-OFDM and Universal Filtered Multi-carrier (UFMC) waveform is proposed to achieve compatibility between different numerology sets. In the design of [7], the UFMC waveform carries a sequence of data with higher subcarrier spacing and is divided into independent sub-bands, while the OFDM waveform carries a lower subcarrier spacing for ordinary transmission. Unlike the combination of CP-OFDM and UFMC waveforms, the authors of [8] proposed the use of filter bank multi-carrier (FBMC) and CP-OFDM waveforms for coexistence. However, the authors pointed out that from the perspective of frequency power density (PSD), FBMC and CP-OFDM waveforms cannot achieve good coexistence because the subcarrier-level filtering process is performed in FBMC. Hence, there is no effective method to distinguish the subcarriers of OFDM and FBMC waveforms. After loading the FBMC waveform, interference that is difficult to eliminate appears in the CP-OFDM waveform, resulting in poor performance. From this perspective, the advantages and disadvantages of the coexistence scheme of FBMC and OFDM cannot be seen. In addition, the authors of [9] conducted a survey and review of possible multi-waveform configuration and multi-numerology set schemes applicable in different application scenarios, pointing out the suitable OFDM and single-carrier frequency division multiple access (SC-FDMA) waveform combinations in LTE, the suitable OFDM and OFDM with index modulation (OFDM-IM) waveform combinations in ultra-reliable low-latency communication (URLLC) scenarios, and the suitable OFDM and FMCW waveform combinations in radar communication fusion scenarios. The literature also proposed that enhanced mobile

broadband (eMBB) services can achieve multi-parameter set configuration through the combination of OFDM, while massive machine type communications (mMTC) services can achieve the goal of multi-waveform configuration and multi-parameter set configuration through loading different types of filters.

This paper presents a new candidate waveform scheme named Generalized FB-OFDM (GFB-OFDM), with a unified structure where it is capable of meeting the requirements of various 6G scenarios. This candidate scheme can be flexibly compatible with single carriers and multi-carriers to form a unified framework for the overall solutions. The method that achieves this compatibility among multiple existing waveform schemes is based on the parameter adjustment of GFB-OFDM, especially through the coordination of two stages of inverse fast Fourier transform (IFFT) processing and the filtering module. When the requirements of different scenarios are set for the air interface, it is possible to achieve corresponding characteristics such as high spectral efficiency, low peak-to-average ratio, low latency, and different numerology between sub-bands with low processing complexity.

The rest of this paper is organized as follows. In Section 2, the system model is detailed. Then, a unified GFB-OFDM structure is described in Section 3. Section 4 shows simulation results. Finally, we offer our conclusion in Section 5.

2. System Model

Considering the GFB-OFDM system, which is illustrated in Figure 1, each group of information bits is first mapped into K amplitude-phase modulation (APM) symbols. Then, the K APM data symbols are divided into G groups, where the g-th group can be denoted as $\boldsymbol{s}_g = \left[s_g(0), \ldots, s_g(K-1)\right]^T$, where $\mathbf{E}[|s_g(i)|^2] = 1$, for all $s_g(i)$ and $g = 0, 1, \ldots, G-1$. Next, two stages of IFFT are applied to process each group of symbols. In the g-th group, $(M_{1,g} - K)$ zero-valued symbols are first inserted into $\boldsymbol{s}_g$, and then, inserted into $M_{1,g}$-point IFFT, yielding the time-domain symbols denoted as $\boldsymbol{s}_{\mathrm{T},g}$, which can be expressed as

$$\boldsymbol{s}_{\mathrm{T},g} = \sqrt{\frac{M_{1,g}}{KG}} F^H_{M_{1,g}} \left[\mathbf{0}^T_{(M_{1,g}-K)/2}, \boldsymbol{s}_g^T, \mathbf{0}^T_{(M_{1,g}-K)/2}\right]^T, \tag{1}$$

where $F^H_{M_{1,g}}$ denotes the $M_{1,g}$-sized inverse DFT IDFT matrix and $\mathbf{0}_{(M_{1,g}-K)/2}$ denotes the $(M_{1,g} - K)/2$-sized vector containing zero-valued symbols. Next, an L_g length CP is added into $\boldsymbol{s}_{\mathrm{T},g}$, giving $\boldsymbol{s}'_{\mathrm{T},g}$. Note here that CP is added to prevent inter-symbol interference. The symbols in $\boldsymbol{s}'_{\mathrm{T},g}$ are parallel-to-serial (P/S) converted and are inserted into the second-level IFFT group by group. Here, the role of P/S is to re-group the outputs of the first-level IFFT processing, so that the corresponding output symbols can be fed into the second-level IFFT processing properly.

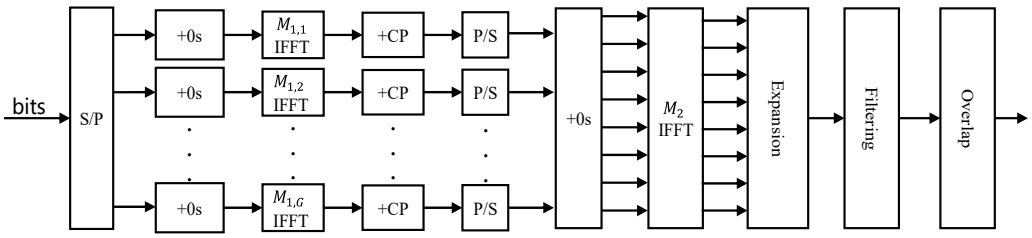

Figure 1. Illustration of the GFB-OFDM transmitter.

In the second level of IFFT processing, (M_2-G) zero-valued symbols are first added into the k-th group of symbols, giving $\boldsymbol{s}'_k$. Then, the k-th group of symbols is inserted into the M_2-point IFFT, yielding the k-th group of transmitted symbols denoted as $\boldsymbol{S}_k$. Next, the transmitted symbols are windowed using a polyphase filter, where the impulse response of the filter arranged in the k-th group be $\boldsymbol{g}_k$, which can be expressed as

$$\boldsymbol{g}_k = [g_k(0), g_k(1), \ldots, g_k(L_{\mathrm{F}} - 1)]^T, \tag{2}$$

where L_F is the length of a prototype filter. Collecting the symbols after the filtering operation, $M_{1,g}$ groups of symbols are overlapped and transmitted into the wireless channel.

As shown in Figure 2, the received symbols are first input into the filter, and then, fed into the M_2-point fast Fourier transform (FFT), yielding the received symbols denoted as $\boldsymbol{Y}$, which can be expressed as

$$\boldsymbol{Y} = \boldsymbol{HS} + \boldsymbol{W}, \tag{3}$$

where $\boldsymbol{H}$ is the channel vector containing the normalized Rayleigh fading coefficients, and $\boldsymbol{W}$ is the complex-valued additive white Gaussian noise (AWGN) vector with zero mean and variation of σ^2. Next, after removing CP and redundant symbols, the received symbols are divided into G groups. The g-th group of received symbols is fed into $M_{1,g}$-point FFT. Finally, after removing the redundant symbols from the outputs, the received symbols are detected according to the maximum likelihood detection [10].

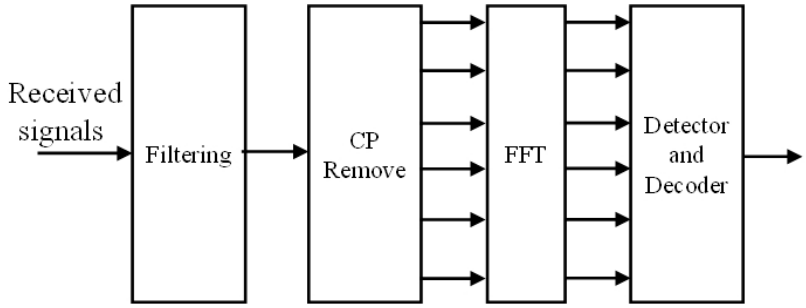

Figure 2. Illustration of the GFB-OFDM receiver.

3. Flexible Waveform Design for GFB-OFDM

In the GFB-OFDM transceiver, module designs are adopted under the unified architecture of the waveform, such as subcarrier selection, sub-band selection, filtering module, and so on. The proposed scheme can achieve the flexible adjustment of parameters such as subcarrier spacing, sub-band bandwidth, and filter length. Thus, various waveform schemes can be achieved according to the specific application scenarios.

3.1. Module Design of Subcarrier Level Processing and Sub-Band Level Processing

In the module design of the GFB-OFDM waveform, a two-stage processing scheme, which is the subcarrier level processing and sub-band level processing, is adopted. In this design, the two-level processing scheme of subcarrier level and sub-band level decomposes the higher-order IFFT/FFT processing into two low levels of IFFT/FFT processing with the same bandwidth configuration, leading to the reduced processing complexity in our GFB-OFDM architecture. In the two-stage IFFT/FFT processing module, different numerologies and asynchronous transmission between sub-bands are supported. By contrast, in order to support different numerologies and asynchronous transmission between sub-bands, each sub-band should be processed separately in the conventional one-level IFFT/FFT processing method, which results in higher processing complexity.

Firstly, with the continuous increase in wireless communication bandwidth in 6G, the maximum number of IFFT/FFT points for existing OFDM waveform becomes excessive. In order to solve the high complexity problem caused by the IFFT/FFT size, we propose a two-level processing scheme of subcarrier level and sub-band level. In this case, the large IFFT/FFT size is decomposed into two smaller IFFT/FFT sizes. The number of subcarrier level IFFT and sub-band level IFFT processing points within the bandwidth range of the sub-band is reduced, leading to the reduction of the processing complexity in the unified architecture design. In detail, in GFB-OFDM, the complexity of the IFFT/FFT processing can be expressed as

$$O\left(\sum_{g=1}^{G} M_{1,g} \log M_{1,g} + M_2 \log M_2\right) \tag{4}$$

where, in comparison, the complexity of the IFFT/FFT processing of the conventional CP-OFDM can be expressed as

$$O(M\log M). \tag{5}$$

Secondly, the proposed method can also reduce the latency for some particular 6G scenarios. For the conventional OFDM system, it is necessary to wait for the time-domain data of the next OFDM symbol to be fully generated. Then, a CP is concatenated to the symbol before starting the transmission of the next OFDM symbol. In the two-stage IFFT processing module, after the first-level IFFT, when a portion of the second-level IFFT is completed, the time-domain data of the next OFDM symbol can be transmitted while processing. For example, in URLLC, when the burst data transmission requirement with low-latency requirements occurs, URLLC data can also be inserted in the middle of a transmitted time-domain signal, which is more conducive to reducing latency.

Thirdly, OFDM can hardly support different numerologies and asynchronous transmission between sub-bands, unless each sub-band is processed separately; that is, each sub-band is processed with full bandwidth and separate filtering at the subcarrier level, which results in higher processing complexity. The unified architecture scheme achieves this advantage by allowing for different temporal data attributes on different sub-bands before the second level of IFFT processing.

3.2. Flexible Design of Waveform Configurations

In the modulation process of the unified architecture, the final waveform structure can be flexibly configured through the different combinations of parameters in two stages of the IFFT module. In the subcarrier level processing module, the number of subcarriers denoted as M and subcarrier spacing for each sub-band can be selected. In the sub-band level processing module, the number of sub-bands G, the bandwidth of sub-bands, and the interval between adjacent sub-bands can be selected according to the restriction of the transmission bandwidth. The various parameters in the sub-band selection module and subcarrier selection module can be flexibly selected according to different scenarios, waveform types, and bandwidth requirements, as shown in the following examples as special cases.

Case I: single-carrier waveform. When the type of waveform with a single carrier is required, the parameters of each module can be selected as $G = 1$ and $K = 1$. With this configuration, processing of the encoded and modulated data in the subcarrier level and the sub-band level module will be relatively simple, or it can be directly skipped in the subcarrier level processing module and sub-band level processing module. In this case, CP can be added to overcome the disadvantages of multipath influences. In addition, guard interval in the frequency domain can also be concatenated as an alternative to CP. In practice, CP or guard interval (GI) can be chosen according to the requirements of scenarios and the channel state information, and then the time-domain symbols are packaged into frames. After the framing operation, those frames are input into the filtering module, which is mainly used to reduce out-of-band leakage in the sub-band and the entire channel and to improve spectral efficiency. For single-carrier waveform, common filtering processing can be selected here.

Case II: CP-OFDM waveform. For the CP-OFDM waveform, the parameters of each module can be selected as $G = 1$ and $K = KG$. The modulated data can be processed by IFFT in the subcarrier level processing module and then sent into the sub-band level processing module, which is relatively simple or can be directly skipped. In the filtering module, if ordinary filtering processing is selected, the waveform structure can become filtered OFDM (F-OFDM), and if windowing processing is selected, it can become W-OFDM. After filtering or windowing, further peak-to-average ratio reduction processing can be performed as needed.

Case III: FB-OFDM waveform. For the filter bank OFDM (FB-OFDM) waveform, the parameters of each module can be selected as $G > 1$ and $K = 1$. The modulated data will be relatively simple in the subcarrier-level processing module, or it can be directly skipped.

In the sub-band level processing module, IFFT operations can be performed, followed by CP/GI and framing operation modules. Then, polyphase filtering processing in the filtering module is selected. Furthermore, in the filtering module, if windowing processing is selected, it can become W-OFDM.

Case IV: GFB-OFDM waveform. In order to meet the requirements for different 6G application scenarios, $G > 1$ and $K > 1$ can be configured for GFB-OFDM. Furthermore, joint processing of the sub-band level IFFT module and filtering module are performed to achieve the GFB-OFDM waveform. Therefore, the GFB-OFDM waveform is flexible by setting different parameter configurations

3.3. Filter Bank Design

In order to improve system efficiency, a polyphase filter is used to filter multiple sub-bands simultaneously in our GFB-OFDM system. First, the output of the sub-band level processing module is fed into the windowing filter module, which includes multiple groups of internal sub-band mixed data. The length of each group of internal sub-band mixed data is consistent and then repeated at the same time. Next, each group of repeated data is multiplied with the time-domain filter function and shifted horizontally backward. Compared with the previous group, the number of shifted bits of each group of the multiplied data is larger than the length of the internal sub-band mixed data before repetition. Finally, the shifted data is vertically superimposed as the output of the windowing filter module.

Since the filter processes each group of the internal sub-band mixed data in a pipeline operation, the GFB-OFDM symbol data output by the windowed filter will contain the last few groups of the previous symbol or the first few groups of the next symbol, which will introduce ISI. In order to eliminate ISI, the last group of the internal sub-band mixed data of this symbol can be copied to the front of the symbol before filtering. When the windowed filter module performs, it shifts and superpositions the output, thus eliminating ISI. Another method is to directly add the same reference symbol sequence at the beginning and end of each symbol. Even if ISI occurs, it can be offset because the internal sub-band mixed data at the beginning and end of each symbol are consistent.

Different filter functions have different effects on the suppression of out-of-band leakage and data demodulation performance. The filter function used in the GFB-OFDM system should separate the signals of different sub-bands. To prevent the data between different sub-bands from interfering with each other, a filter function with small out-of-band leakage should be designed. In this study, we consider a root-raised cosine pulse with a roll-off factor of one, and thus we have

$$g(t) = \sqrt{\delta(\cos 2\pi t\delta + 1)} \tag{6}$$

if $-1/2\delta \leq t \leq 1/2\delta$, or $g(t) = 0$ otherwise.

4. Simulation Results

In 6G, there will be coexistence and rapid switching among multiple scenarios and the GFB-OFDM waveform can adjust to the appropriate parameters dynamically according to the specific requirements for the purpose scheme. In this section, the parameters of GFB-OFDM waveform adaptation are designed for the actual scenarios such as a single parameter set in one scenario, or multiple parameter settings in the coexistence scenario of industrial automation control applications and common mobile service applications. Then, preliminary performance simulation verification is carried out. The automation control of industrial operation in wireless communication is an important scenario of URLLC in 5G NR. Strengthening the integration of wireless communication and industrial applications is also an important scenario for 6G. Some industrial applications have high-reliability and low-latency requirements, and these services are always burst and the scale of data volume is not large. If a frequency band is dedicated to the industrial application, the utilization of spectrum resources is not high because of the small amount of data. If the dedicated band

bandwidth is relatively narrow, it is difficult to meet the needs of low-latency and burst services. Therefore, it is necessary to share the same frequency band with high-reliability and low-delay services in industrial applications to improve spectrum utilization.

In order to meet the low-latency requirements, OFDM symbols will be shorter. In order to meet various burst traffic requirements, the transmission bandwidth of different subcarrier spacings will change rapidly. When there is no URLLC burst traffic, ordinary wireless communication traffic is normally transmitted, and the subcarrier spacing is small, we test this scenario first using the simulation parameters shown in Table 1. When there is URLLC burst traffic, the ordinary wireless communication traffic of the symbol is replaced by the burst traffic, and the subcarrier spacing becomes larger. The replaced ordinary wireless communication service can be transmitted through retransmission. The existing 5G NR waveform cannot support the rapid change of the transmission bandwidth of different subcarrier spacings, while the GFB-OFDM waveform can flexibly support the change of transmission bandwidth by changing the number of sub-bands parameter; we test this scenario in order to show the bit error rate of GFB-OFDM. Moreover, the two-stage IFFT can reduce the delay. In addition, short OFDM symbols can be inserted in the middle of long OFDM symbols to further reduce the delay.

Table 1. Simulation parameters.

Parameters	Values
Subcarrier spacing	15, 30, 60 kHz
Number of sub-bands	4
Number of subcarriers	16, 32, 64, 64
IFFT sizes	32, 64, 128, 128
CP length	8
Filtering type	dual root-raised cosine
Filter length	40
Filter parameters	[0.1, 0.1]

For the eMBB conventional wireless communication scheme, burst low-latency applications in URLLC, and machine-type communication scheme in mMTC, different sub-band parameters are set separately. In order to facilitate the stacking and transmission of data in this simulation, the bandwidth of different sub-bands is set to a fixed value, and different subcarrier spacings are achieved by different IFFT points within the sub-band. For conventional wireless communication applications, 128-point IFFT is adopted, with a bandwidth of 2 MHz and subcarrier spacing of 15 kHz. For burst low-latency applications, 32-point IFFT with a bandwidth of 2 MHz and subcarrier spacing of 60 kHz are set. For machine-type communication applications, 64-point IFFT with a bandwidth of 2 MHz and a subcarrier interval of 30 kHz are set. In the three scenarios, the GFB-OFDM waveform is used for transmission, and the transmission performance is compared with the corresponding parameters of the CP-OFDM waveform. The bit error rate of the eMBB scenario is shown in Figure 3 for the AWGN channel and Figure 4 for the Rayleigh channel.

Similarly, when the IFFT points of each sub-band are set to 64, subcarrier spacing will change to 30 kHz, which is set for mMTC. The simulation results are shown in Figure 5. When the IFFT points of each sub-band are set to 32, subcarrier spacing will change to 60 kHz, which is set for URLLC. The simulation results are shown in Figure 6. It should be noted that when different subcarrier intervals are used to meet the transmission rate and delay requirements of different scenarios, larger subcarrier spacings introduce more zeros between frequency domain samples. Therefore, in scenarios with larger subcarrier spacings, lower BER can be achieved.

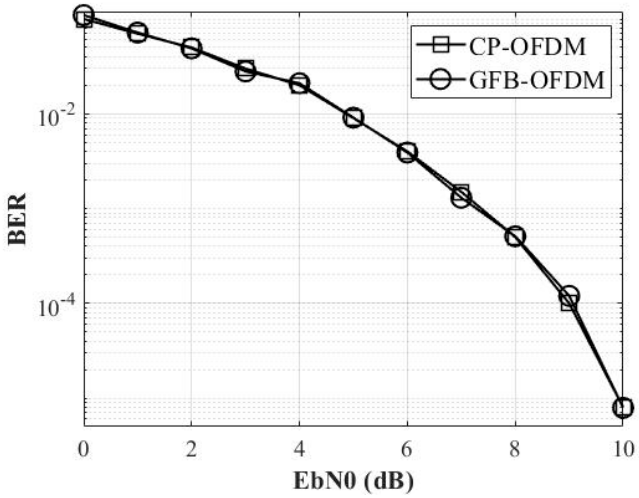

Figure 3. BER of GFB−OFDM with SCS = 15 kHz, compared with CP−OFDM, when communicating over AWGN channel.

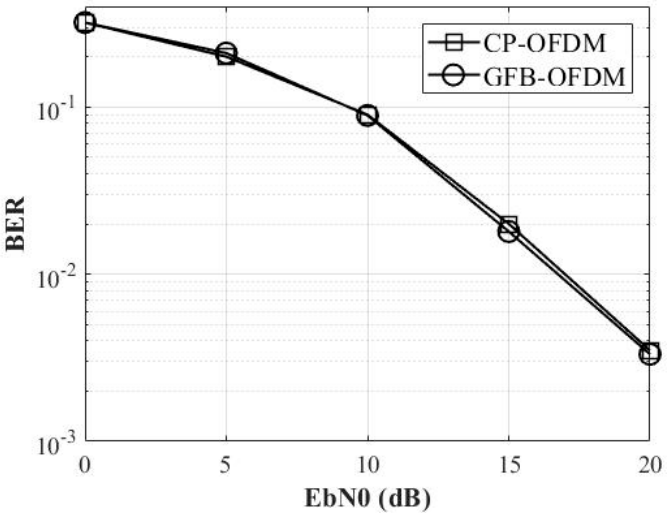

Figure 4. BER of GFB−OFDM with SCS = 15 kHz, compared with CP−OFDM, when communicating over Rayleigh channel.

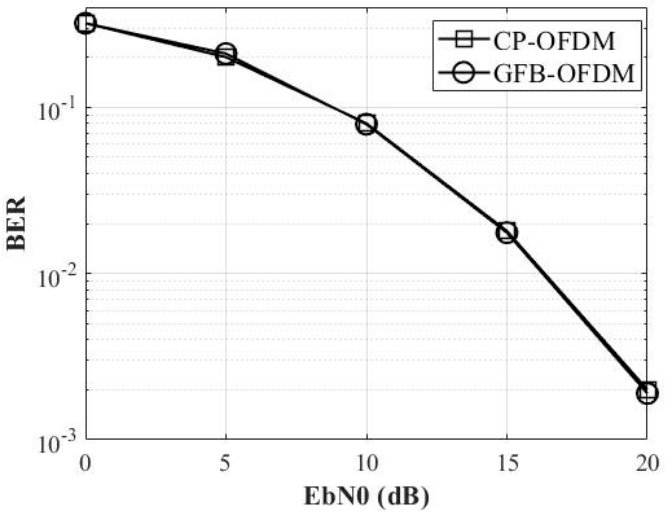

Figure 5. BER of GFB−OFDM with SCS = 30 kHz, compared with CP−OFDM, when communicating over Rayleigh channel.

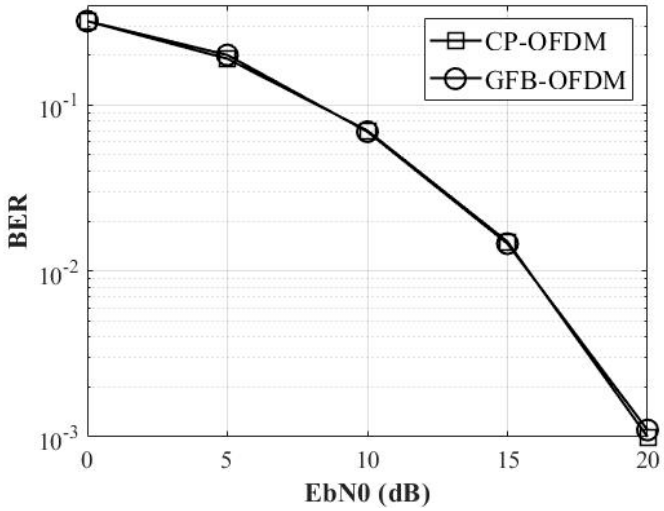

Figure 6. BER of GFB−OFDM with SCS = 60 kHz, compared with CP−OFDM, when communicating over Rayleigh channel.

As shown in Figures 5 and 6, when the data in each sub-band are under different configurations, GFB-OFDM can achieve similar BER performance to CP-OFDM in the Rayleigh channel. It should be noted that different configurations in two sub-bands are set for GFB-OFDM, while OFDM is set with one sub-band with equal bandwidth to GFB-OFDM, which is because different configurations for OFDM will destroy the orthogonality of subcarriers in OFDM. Hence, our work focuses on the feasibility of GFB-OFDM when different configurations are set.

In Figure 7, the IFFT/FFT operation complexity of GFB-OFDM and CP-OFDM is shown. We can see that the IFFT/FFT operation complexity of GFB-OFDM is lower than that of the conventional CP-OFDM system when the total number of subcarriers is the same. Furthermore, it can be shown that by carefully designing the group size G and two-level IFFT/FFT sizes, the operational complexity can be reduced.

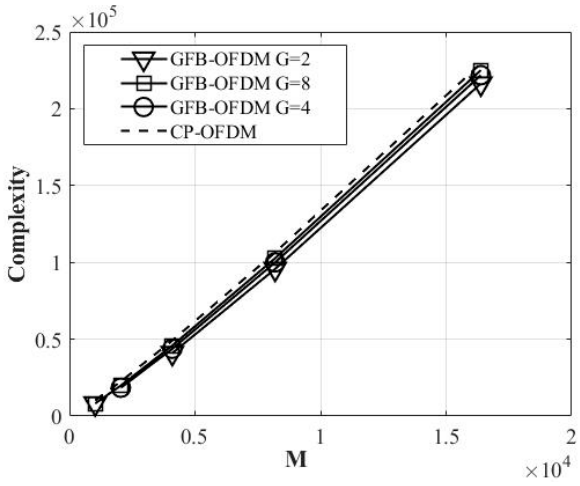

Figure 7. IFFT/FFT complexity of GFB−OFDM and CP−OFDM.

In summary, it can be concluded that when GFB-OFDM and CP-OFDM are used with the same bandwidth consideration and IFFT points to achieve the same subcarrier spacing, the signal-to-noise ratio improvement required for GFB-OFDM and CP-OFDM waveforms to achieve the same BER is almost the same. When there is a coexistence of three scenarios, the simulation is based on the coexistence of URLLC traffic, ordinary wireless communication traffic, and mMTC. In this situation, the coexistence of subcarrier

spacings with different sizes will share the same frequency band, which further leads to the loss of orthogonality between subcarriers. In order to avoid the excessive increase in the complexity of the receiver, one way is to limit the subcarrier spacing of different sizes to a fixed sub-band and realize the coexistence of different subcarrier spacings by adjusting the sub-band.

5. Conclusions

In this study, a generalized architecture of waveform named GFB-OFDM for 6G is proposed in order to meet the requirements of different scenarios with one flexible architecture. The mathematical formulation of GFB-OFDM is provided on both the transmitter and the receiver side. Furthermore, the two stages of IFFT in unified architecture are proposed, and a detailed description of the basic implementations of core modules is exemplified in this article. Moreover, the BER performance of GFB-OFDM versus OFDM in the Rayleigh channel is studied. Our study shows that the GFB-OFDM can achieve similar BER performance when considering different numerologies. Moreover, the performance of GFB-OFDM remains stable and achieves less complexity because of the polyphase filter compared with that of OFDM. As a result, the output data in different sub-bands are clearly separated through two stages of IFFT structure and polyphase filter, which is similar to the result that the data in different sub-bands are filtered or windowed, respectively, with different scales of filter. Hence, the proof of this similarity is our future research, which is also helpful in reducing the complexity of the receiver mentioned in this study.

Author Contributions: Conceptualization, Y.X. and H.Z.; methodology, T.B.; software, J.H.; validation, T.B.; formal analysis, J.H.; investigation, Y.X.; resources, T.B.; data curation, J.H.; writing—original draft preparation, H.Z.; writing—review and editing, Y.X.; visualization, T.B.; supervision, H.Z.; project administration, T.B.; funding acquisition, Y.X. All authors have read and agreed to the published version of the manuscript.

Funding: This research was funded by ZTE Industry-University-Institute Cooperation Funds under Grant No. HC-CN-20220616006.

Data Availability Statement: Data are unavailable due to privacy.

Conflicts of Interest: Author Yu Xin, Tong Bao, Jian Hua were employed by the company ZTE Corporation. The remaining authors declare that the research was conducted in the absence of any commercial or financial relationships that could be construed as a potential conflict of interest.

References

1. Saad, W.; Bennis, M.; Chen, M. A vision of 6G wireless systems: Applications, trends, technologies, and open research problems. *IEEE Netw.* **2020**, *34*, 134–142. [CrossRef]
2. Mohjazi, L.; Selim, B.; Tatipamula, M.; Imran, M.A. The Journey Toward 6G: A Digital and Societal Revolution in the Making. *IEEE Internet Things Mag.* **2024**, *7*, 119–128. [CrossRef]
3. Hazra, A.; Munusamy, A.; Adhikari, M.; Awasthi, L.K.; Venu, P. 6G-Enabled Ultra-Reliable Low Latency Communication for Industry 5.0: Challenges and Future Directions. *IEEE Commun. Stand. Mag.* **2024**, *8*, 36–42. [CrossRef]
4. Demir, A.F.; Arslan, H. Inter-numerology interference management with adaptive guards: A cross-layer approach. *IEEE Access* **2020**, *8*, 30378–30386. [CrossRef]
5. Zaidi, A.A.; Baldemair, R.; Tullberg, H.; Bjorkegren, H.; Sundstrom, L.; Medbo, J.; Kilinc, C.; Da Silva, I. Waveform and numerology to support 5G services and requirements. *IEEE Commun. Mag.* **2016**, *54*, 90–98. [CrossRef]
6. Zhang, X.; Zhang, L.; Xiao, P.; Ma, D.; Wei, J.; Xin, Y. Mixed numerologies interference analysis and inter-numerology interference cancellation for windowed OFDM systems. *IEEE Trans. Veh. Technol.* **2018**, *67*, 7047–7061. [CrossRef]
7. Hammoodi, A.; Audah, L.; Aljumaily, M.S.; Taher, M.A.; Shawqi, F.S. Green coexistence of CP-OFDM and UFMC waveform for 5G and beyond systems. In Proceedings of the 2020 4th International Symposium on Multidisciplinary Studies and Innovative Technologies (ISMSIT), Istanbul, Turkey, 22–24 October 2020; pp. 1–6.
8. Bodinier, Q.; Bader, F.; Palicot, J. On spectral coexistence of CP-OFDM and FB-MC waveform in 5G networks. *IEEE Access* **2017**, *5*, 13883–13900. [CrossRef]

9. Ankarali, Z.E.; Peköz, B.; Arslan, H. Flexible radio access beyond 5G: A future projection on waveform, numerology, and frame design principles. *IEEE Access* **2017**, *5*, 18295–18309. [CrossRef]
10. Zhang, H.; Yang, L.-L.; Hanzo, L. Compressed sensing improves the performance of subcarrier index-modulation-assisted OFDM. *IEEE Access* **2016**, *4*, 7859–7873. [CrossRef]